Environmental Science Nano

PAPER

Cite this: *Environ. Sci.: Nano*, 2017, 4, 2018

Comprehensive evaluation of the cytotoxicity of CdSe/ZnS quantum dots in *Phanerochaete chrysosporium* by cellular uptake and oxidative stress

Liang Hu,[ab] Jia Wan,[ab] Guangming Zeng,*[ab] Anwei Chen,*[c] Guiqiu Chen,[ab] Zhenzhen Huang,[ab] Kai He,[ab] Min Cheng,[ab] Chengyun Zhou,[ab] Weiping Xiong,[ab] Cui Lai[ab] and Piao Xu[ab]

Received 9th June 2017,
Accepted 18th August 2017

DOI: 10.1039/c7en00517b

rsc.li/es-nano

The growing potential of quantum dots (QDs) in biological and biomedical applications has raised considerable concern due to their toxicological impact. Consequently, it is urgent to elucidate the underlying toxicity mechanism of QDs. In this work, we comprehensively investigated the cellular uptake of four CdSe/ZnS QDs (COOH CdSe/ZnS 525, COOH CdSe/ZnS 625, NH_2 CdSe/ZnS 525, and NH_2 CdSe/ZnS 625) and induced physiological responses in *Phanerochaete chrysosporium* (*P. chrysosporium*) through inductively coupled plasma optical emission spectroscopy, confocal laser scanning microscopy, and the determination of malondialdehyde content, superoxide level, superoxide dismutase activity, catalase activity and glutathione level. The results showed that the four CdSe/ZnS QDs accumulated largely in the hyphae and caused oxidative stress to *P. chrysosporium* in the tested concentration range (10–80 nM). Furthermore, the cellular uptake and cytotoxicity were related to the physicochemical properties of the QDs, such as particle size and surface charges. Negatively charged CdSe/ZnS QDs with small size could be more easily ingested by *P. chrysosporium* than large ones; thus small size CdSe/ZnS QDs were more cytotoxic to *P. chrysosporium*. On the other hand, small negatively charged CdSe/ZnS QDs resulted in greater cytotoxicity than large negatively charged CdSe/ZnS QDs. The obtained results offer valuable information for revealing the toxicity mechanism of QDs in living cells.

Environmental significance

QDs are expected to have an important impact on biomedicine, although they still need to overcome side effects before they can be widely used. Exploring the molecular interaction of QDs in the cellular environment is crucial for their application. Therefore, the responsible mechanism for QD internalization has attracted great attention in scientific circles. Here we comprehensively investigated the cellular uptake of four CdSe/ZnS QDs and induced physiological responses in *Phanerochaete chrysosporium*, revealing the toxicity mechanism of QDs in living cells.

1. Introduction

Quantum dots (QDs) are generally made up of atoms from IIIA–VA or IIB–VIA elements in the chemical periodic table.[1] A semiconductor core (*e.g.*, CdS, CdSe, and CdTe) which can be encapsulated in a shell (*e.g.*, ZnS) to enhance both electronic and optical properties and reduce core metal leaching is the main structure of a typical QD.[2,3] QDs are also among the most promising fluorescent nanoparticles for biological and biomedical applications because of their unique photophysical properties, such as high brightness, tunable broad excitation coupled with narrow emission spectra, and excellent photostability.[4–8] With the recent development of bioconjugate techniques and surface modification, QDs have been extensively applied to *in vitro* and *in vivo* imaging, virus and cell tracing, cellular protein labelling, targeted drug delivery, and cancer therapy.[9–11] However, the comprehensive toxicity evaluation of QDs is of special significance for clinical medicine due to their heavy metal components and nanosize effects.

Although the potential toxicity of QDs has remained a large controversy in biomedical applications and a challenge

[a] *College of Environmental Science and Engineering, Hunan University, Changsha, Hunan 410082, P.R. China. E-mail: zgming@hnu.edu.cn; Fax: +86 731 88823701; Tel: +86 731 88822829*
[b] *Key Laboratory of Environmental Biology and Pollution Control (Hunan University), Ministry of Education, Changsha, Hunan 410082, P.R. China*
[c] *College of Resources and Environment, Hunan Agricultural University, Changsha, Hunan 410128, P.R. China. E-mail: A.Chen@hunau.edu.cn*

for clinical studies, many toxicological studies on QDs have been implemented for this purpose.[12,13] It has been verified that the cytotoxicity of QDs would lead to cell growth inhibition, mitochondrial dysfunction, DNA damage, and apoptosis.[14–16] The physicochemical properties of QDs, including the core composition, size, surface charge, and functionalization, would influence their cytotoxicity to a great extent.[17] For example, Li *et al.*[18] reported that CdSe QDs were more cytotoxic than CdSe/ZnS QDs with the same size and functionalization, indicating that a cadmium-induced cytotoxic response could be decreased by encapsulating the core with a shell. This finding was further supported by Su *et al.*,[19] who showed that CdTe/ZnS QDs were less cytotoxic as compared to CdTe QDs. In the same way, Domingos *et al.*[20] reported that CdTe QDs capped with surfactant were more cytotoxic than CdTe/ZnS QDs coated with polyethylene glycol (PEG) to *Chlamydomonas reinhardtii* cells. In regard to size effects, Soenen *et al.*[21] found that the cellular uptake and subcellular distribution of CdTe QDs changed dramatically with the size of QDs. There are also some studies which showed that the surface charge of QDs could affect their cytotoxicity,[15,22] with positively charged QDs being more cytotoxic than negatively charged QDs.[15] Additionally, the QDs' functionalization could alleviate the induced cytotoxicity as well.[23,24]

To further explore and understand the cytotoxicity of QDs, many research groups have focused their attention on the study of its mechanism.[12,13,25] It has been widely deemed that the release of toxic cadmium ions (Cd^{2+}) and the generation of reactive oxygen species (ROS) are the main reasons responsible for the cytotoxicity of QDs.[14,26,27] Since Cd^{2+} can be released through the oxidation of QDs and bind to the sulfhydryl groups in many intracellular proteins, it may result in the functionality reduction of various subcellular organelles.[20,28] QD-induced ROS have been verified to cause metabolic function loss, DNA nicking and breakage, and apoptosis.[9,10,29] However, it is difficult to thoroughly understand the potential cytotoxicity mechanism of QDs since the cytotoxicity caused by QDs is extremely complicated. Little consensus can be reached. Although each of the above studies has provided valuable information on the influence of a given property of QDs (*i.e.*, core composition, size, surface charge, and functionalization), a comparative analysis is necessary to determine the extent to which each of these properties causes cellular responses in isolation or in combination. It is still unclear which specific properties of QDs lead to induced physiological responses.

In view of this, four types of CdSe/ZnS QDs were employed in this study as different types of pollutants to investigate their cellular uptake and induced physiological responses in *Phanerochaete chrysosporium* (*P. chrysosporium*), which has been widely used in treating wastewater containing toxic organic pollutants and heavy metals because of its excellent ability to degrade organic pollutants and absorb heavy metals.[30–32] As *P. chrysosporium* was sensitive to xenobiotics and it could quickly respond to changes in the surrounding environment, *P. chrysosporium* was used as the target organism to explore the cytotoxicity of QDs. Moreover, studies on the physiological responses of *P. chrysosporium* under QD exposure are still limited. Particularly, the effects of incubation concentration and exposure time to QDs on the cellular uptake and oxidative stress in *P. chrysosporium* have not been reported in the literature yet. Consequently, simultaneous analysis of the cellular uptake and physiological responses in *P. chrysosporium* is conducted to achieve a reliable and comprehensive evaluation on the biosafety of QDs.

2. Materials and methods

2.1. Reagents and instruments

The QDs used in this work were purchased from Wuhan Jiayuan Quantum Dots Company (Wuhan, China). The nanoparticles were preserved as 8 μM QD in 200 μL borate buffer solutions. The four CdSe/ZnS QDs (COOH CdSe/ZnS 525, COOH CdSe/ZnS 625, NH_2 CdSe/ZnS 525, and NH_2 CdSe/ZnS 625) consist of a cadmium selenide (CdSe) core and a zinc sulfide (ZnS) shell, which is encapsulated with a uniform amphipathic polymer PEG coating. Their differences include particle size and surface functional groups, *i.e.* $-NH_2$ and –COOH. In this work, all reagents must be of analytical reagent grade and were purchased from Sigma (St. Louis, MO, USA). Ultrapure water produced by a Milli-Q system (18.25 MΩ cm^{-1}, Millipore, France) was used throughout the process. To control the blank value, the experiment ware was completely washed by soaking in 10% nitric acid (HNO_3) for at least 24 h.

The CdSe/ZnS QDs were characterized by photoluminescence (PL) spectroscopy, high-resolution transmission electron microscopy (HRTEM), and dynamic light scattering (DLS), respectively. All optical measurements were carried out at room temperature under ambient air conditions. PL measurements were performed using a HORIBA JOBTN YVON FLUOROMAX-4 spectrofluorimeter. The PL quantum yield (QY) of the samples was estimated using Rhodamine 6G (QY = 95%) in ethanol solution as a reference standard, which was freshly prepared to decrease the measurement error.[33] The HRTEM overview images were recorded with a Philips CM 200 electron microscope (JEOL JEM-3010, Japan) operated at 200 kV. DLS analysis (hydrodynamic diameter and zeta (ζ) potential) was carried out using a DynaPro Dynamic Light Scatterer (Malvern Instruments).

2.2. *P. chrysosporium* culture

P. chrysosporium has been selected as the target microbe due to its extensive utilization in wastewater decontamination. *P. chrysosporium* BKMF-1767 (ATCC 24725) was obtained from the China Center for Type Culture Collection (Wuhan, China). The fungal spores were prepared by subculturing on potato dextrose agar slants (20.0 g L^{-1} glucose, 20.0 g L^{-1} agar, 3.0 g L^{-1} KH_2PO_4, and 1.5 g L^{-1} $MgSO_4{\cdot}7H_2O$) in a sterilization work station, and then these potato dextrose agar slants were placed in a humid incubator at 37 °C for 7 days.

The fungal spore suspensions were adjusted to 2.0×10^6 CFU mL^{-1} using a turbidimeter (WGZ-200, Shanghai, China). 3 mL of aqueous suspensions of fungal spores were inoculated into 200 mL Kirk's liquid culture medium at 37 °C for 3 days.[34]

2.3. Inductively coupled plasma optical emission spectroscopic analysis

0.2 g of *P. chrysosporium* pellets was seeded into 10 mL centrifuge tubes containing fresh borate buffer solutions with CdSe/ZnS QDs. Then these centrifuge tubes were placed in an orbital shaker (120 rpm) at 37 °C. After 24 h of exposure, the *P. chrysosporium* pellets were harvested and washed three times with ultrapure water, and then the pellets were digested with 4 mL concentrated HNO_3 (67%) for 4 h at 85 °C. The solution was evaporated to remove superfluous acid and diluted with 5 mL HNO_3 (5%) for inductively coupled plasma optical emission spectroscopic (ICP-OES, Optima 5300 DV) analysis. The blank sample was the *P. chrysosporium* pellets without CdSe/ZnS QD exposure. In this work, the uptake amount of CdSe/ZnS QDs was calculated from Cd or Se measured by ICP-OES.

2.4. *P. chrysosporium* uptake of CdSe/ZnS QDs

2.4.1. Incubation concentrations. 0.2 g of *P. chrysosporium* pellets was seeded into 10 mL centrifuge tubes and fresh borate buffer solutions containing different concentrations of CdSe/ZnS QDs (0, 10, 20, 50, and 80 nM) were added. Then these centrifuge tubes were placed in an orbital shaker (120 rpm) at 37 °C. After 24 h of exposure, the *P. chrysosporium* pellets were collected and washed three times with ultrapure water. The uptake of CdSe/ZnS QDs by *P. chrysosporium* was determined as described above.

2.4.2. Incubation time. 0.2 g of *P. chrysosporium* pellets was seeded into 10 mL centrifuge tubes and fresh borate buffer solutions containing different concentrations of CdSe/ZnS QDs (0, 10, 20, 50, and 80 nM) were added. Then these centrifuge tubes were placed in an orbital shaker (120 rpm) at 37 °C. After incubation for different durations (0, 3, 6, 9, 15, and 24 h), the *P. chrysosporium* pellets were collected and washed three times with ultrapure water. The uptake of CdSe/ZnS QDs by *P. chrysosporium* was determined as described above.

2.5. Confocal laser scanning microscopy

0.2 g of *P. chrysosporium* pellets was seeded into 10 mL centrifuge tubes and 5 mL 2,7-dichlorodihydrofluorescein-diacetate (H_2DCF-DA) (5 μM) was added into the incubation solution for 2 h. Afterward, the medium was discarded, and the pellets were treated with different concentrations of CdSe/ZnS (0, 10, 20, 50, and 80 nM) for 24 h. Then the pellets were washed with fresh phosphate-buffered saline (PBS) three times for confocal laser scanning microscopy analysis (FV1000, TY1318, Japan; equipped with a double photon detector).

2.6. Lipid peroxidation and superoxide (O_2^-) production

Lipid peroxidation was determined by measuring the content of malondialdehyde (MDA), which is generally used as the indicator of lipid peroxidation and free radical production.[35] The MDA content was measured *via* the thiobarbituric acid (TBA) reaction according to the method reported by Aravind and Prasad.[36] The harvested *P. chrysosporium* pellets were homogenized in a 10 mL centrifuge tube with 10% trichloroacetic acid and centrifuged at 10 000 rpm for 20 min at 4 °C. Then the supernatant was separated and boiled with TBA for 20 min. The heated supernatant was centrifuged at 8000 rpm for 10 min, and the absorbance was recorded at 532 and 600 nm using a UV-vis spectrophotometer (Model UV-2550, Shimadzu, Japan).

O_2^- production was measured according to the method reported by Lei *et al.*[37] The harvested *P. chrysosporium* pellets were homogenized in a 10 mL centrifuge tube with 50 mM PBS (pH 7.8) and centrifuged at 10 000 rpm for 15 min at 4 °C. Then 1 mL of the supernatant was mixed with 0.9 mL of 50 mM PBS (pH 7.8) and 0.1 mL of 10 mM hydroxylamine hydrochloride. The reaction system was placed in a water bath at 25 °C for 20 min before adding 1 mL of 7 mM α-naphthylamine and 1 mL of 17 mM *p*-aminobenzenesulfonic acid. Afterward, the absorbance of the above mixture was recorded at 530 nm.

2.7. Antioxidant enzyme analysis

Superoxide dismutase (SOD) (converts superoxide to hydrogen peroxide) activity was determined according to the method described in our previous work.[35] *P. chrysosporium* pellets were collected by centrifugation and homogenized in 0.05 M PBS (pH 7.8). Then the homogenate was centrifuged at 10 000 rpm for 15 min at 4 °C, and the supernatant was separated for enzyme assay. SOD activity was measured by monitoring the inhibition of photochemical reduction of nitroblue tetrazolium chloride (NBT) in a reaction system containing 2.25 mM NBT, 200 mM methionine, 1 M Na_2CO_3, 60 mM riboflavin, 3 nM EDTA, and 0.1 M PBS (pH 7.8). The absorbance was recorded at 560 nm.

Catalase (CAT) (converts hydrogen peroxide to oxygen and water) activity was assayed in a 3 mL reaction system containing 20 mM H_2O_2, 50 μL enzymatic extract, and 50 mM PBS (pH 7.8), according to the method described by Cavalcanti *et al.*[38] CAT activity was evaluated by measuring the rate of decrease in absorbance at 240 nm (molar extinction coefficient $\varepsilon = 36.6\ mM^{-1}\ cm^{-1}$).

2.8. Measurement of glutathione levels

Glutathione levels were measured using 5,5-V-dithiobis-(2-nitrobenzoic acid)-glutathione disulfide according to the method reported by Rehman and Anjum.[39] The harvested *P. chrysosporium* pellets were rinsed with PBS (0.1 M, pH 7.0) plus 0.5 mM EDTA and sonicated in a 10 mL centrifuge tube with an ice-water bath. The samples were sonicated for 5 s in intervals of 8 s with a total time of 5 min. The sonication was

carried out with the output power of 400 W for each sample. The suspension was centrifuged at 15 000 rpm for 10 min at 4 °C, and the supernatant was used for measuring the concentration of glutathione. Reduced glutathione (GSH) was determined by adding 2.0 mL PBS to 0.5 mL of the above supernatant, followed by adding 0.5 mL of 3 mM 5-dithio-bis-(2-nitrobenzoic acid). After 5 min reaction, the absorbance was recorded at 412 nm.

3. Results and discussion

3.1. The physicochemical characteristics of CdSe/ZnS QDs

In an attempt to explore the individual and/or collective roles of various physicochemical properties of CdSe/ZnS QDs, a range of CdSe/ZnS QD sizes, surface charges, and functional groups was investigated. Specifically, four types of CdSe/ZnS QDs with maximum luminescent wavelengths of 525 nm, 625 nm, 525 nm, and 625 nm were used in this experiment. With an excitation wavelength of 380 nm, COOH CdSe/ZnS 525, COOH CdSe/ZnS 625, NH_2 CdSe/ZnS 525, and NH_2 CdSe/ZnS 625 present a fluorescence emission maximum at 524 nm, 620 nm, 522 nm, and 624 nm (Table 1), respectively, indicating that the four types of CdSe/ZnS QDs are nearly monodisperse and homogeneous. The physical diameters of COOH CdSe/ZnS 525, COOH CdSe/ZnS 625, NH_2 CdSe/ZnS 525, and NH_2 CdSe/ZnS 625 determined by HRTEM are 5.2 ± 0.3, 10.4 ± 1.1, 5.4 ± 0.5, and 10.3 ± 0.9 nm (Fig. 1), respectively, which are smaller than those (22.3 ± 5.4, 30.1 ± 3.6, 17.6 ± 3.5, and 27.8 ± 2.5 nm) determined by DLS. The deviation of the diameters measured by HRTEM from those measured by DLS is attributed to different surface states of nanoparticles under the tested conditions.[40,41] QD samples are directly measured in the aqueous phase for DLS analysis while the solution must be strictly evaporated in HRTEM characterization. The zeta (ζ) potentials of COOH CdSe/ZnS 525, COOH CdSe/ZnS 625, NH_2 CdSe/ZnS 525, and NH_2 CdSe/ZnS 625 are −12.9 ± 1.1, −15.2 ± 1.4, −6.7 ± 0.6, and −9.6 ± 0.7 mV, respectively. Thus, COOH CdSe/ZnS QDs possess more negative charges than NH_2 CdSe/ZnS QDs. In addition, the amount of Cd and Se atoms in a single QD nanoparticle ($N_{Cd/QD}$ and $N_{Se/QD}$) was determined by ICP-OES (Table 1).

3.2. *P. chrysosporium* uptake of CdSe/ZnS QDs

3.2.1. Incubation concentrations. The cellular uptake process plays a key role in the function of QDs in biomedical applications and their health risks. In this study, *P. chrysosporium* pellets were incubated with different concentrations of COOH CdSe/ZnS 525, COOH CdSe/ZnS 625, NH_2 CdSe/ZnS 525, and NH_2 CdSe/ZnS 625 (10, 20, 50, and 80 nM for each QD) for 24 h, and the cellular uptake of CdSe/ZnS QDs was determined by ICP-OES. As shown in Fig. 2a, the uptake by *P. chrysosporium* increased gradually with the increase of incubation concentration for all four types of CdSe/ZnS QDs. With the increased concentration of QDs, the amount of CdSe/ZnS QDs in the cell membrane increased, leading to the increased uptake of CdSe/ZnS QDs by *P. chrysosporium*. However, the cellular uptake of different CdSe/ZnS QDs was distinctly different under identical conditions. For example, the cellular uptake of NH_2 CdSe/ZnS 525 reached 292.3 pmol g^{-1} biomass when the incubation concentration was 80 nM, which was greater than those of NH_2 CdSe/ZnS 625 (166.5 pmol g^{-1} biomass), COOH CdSe/ZnS 525 (101.2 pmol g^{-1} biomass), and COOH CdSe/ZnS 625 (67.5 pmol g^{-1} biomass). Among the four types of CdSe/ZnS QDs, the uptake by *P. chrysosporium* decreased as follows: NH_2 CdSe/ZnS 525 > NH_2 CdSe/ZnS 625 > COOH CdSe/ZnS 525 > COOH CdSe/ZnS 625, which suggests greater uptake of amino-QDs by *P. chrysosporium*. The result may be attributed to amino-QDs possessing less negative surface charges (−6.7 ± 0.6 and −9.6 ± 0.7 mV) than carboxyl-QDs (−12.9 ± 1.1 and −15.2 ± 1.4 mV). Due to the electrostatic repulsion caused by the negative charges on the cell membrane, the more negative surface charges made it more difficult for carboxyl-QDs to adsorb on the cell membrane.[22] In addition, the result also indicated greater uptake by *P. chrysosporium* when treated with smaller QDs (NH_2 CdSe/ZnS 525 and COOH CdSe/ZnS 525). This is because smaller CdSe/ZnS QDs are more easily taken in by *P. chrysosporium*.[42] Due to their small size, CdSe/ZnS QDs can directly enter into the hyphae by several approaches such as macropinocytosis, caveolae-mediated endocytosis, and clathrin-mediated endocytosis.[43] Meanwhile, as endocytosis is an energy-consuming process, smaller CdSe/ZnS QDs would consume less energy than larger CdSe/ZnS QDs, leading to higher uptake.[44] As shown in Fig. 2b, the same results were also observed by determining the Se concentration, which confirmed the accuracy of the employed ICP-OES measurement. Fig. 2c and d show that there is a good linear correlation between CdSe/ZnS QD uptake and the incubation concentration in the medium, indicating that the cellular uptake was a dose-dependent process.

3.2.2. Incubation time. The incubation time plays a vital role in the uptake of QDs by *P. chrysosporium*. The cellular uptake by *P. chrysosporium* exposed to COOH CdSe/ZnS 525, COOH CdSe/ZnS 625, NH_2 CdSe/ZnS 525, and NH_2 CdSe/ZnS

Table 1 The physicochemical properties of four CdSe/ZnS QDs

QDs	Functional group	$\lambda_{emission}$ (nm)	Physical diameter (nm)	Hydrodynamic diameter (nm)	Zeta potential (mV)	$N_{Cd/QD}$	$N_{Se/QD}$
COOH-QDs 525	COOH	524	5.2 ± 0.3	22.3 ± 5.4	−12.9 ± 1.1	165 ± 4	28 ± 5
COOH-QDs 625	COOH	620	10.4 ± 1.1	30.1 ± 3.6	−15.2 ± 1.4	1240 ± 36	359 ± 24
NH_2-QDs 525	NH_2	522	5.4 ± 0.5	17.6 ± 3.5	−6.7 ± 0.6	174 ± 7	32 ± 3
NH_2-QDs 625	NH_2	624	10.3 ± 0.9	27.8 ± 2.5	−9.6 ± 0.7	1263 ± 45	343 ± 33

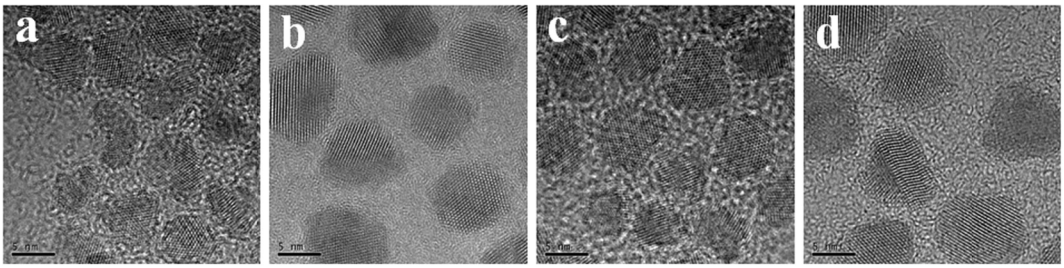

Fig. 1 High-resolution TEM images of COOH CdSe/ZnS 525 (a), COOH CdSe/ZnS 625 (b), NH_2 CdSe/ZnS 525 (c), and NH_2 CdSe/ZnS 625 (d), respectively.

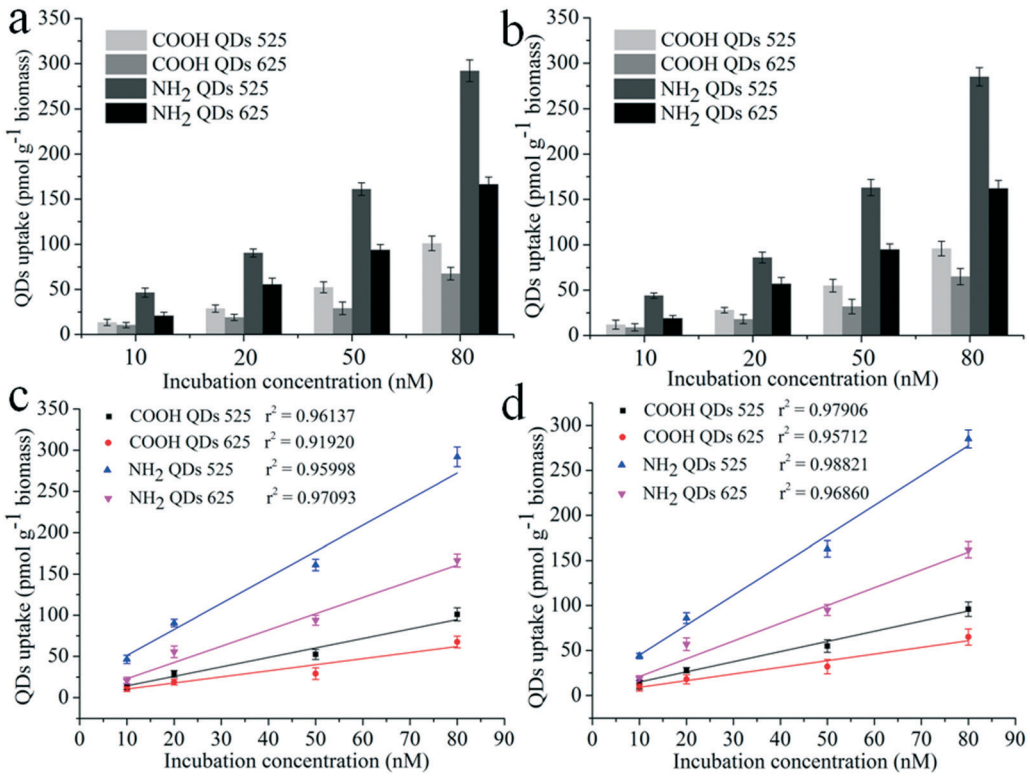

Fig. 2 Cellular uptake of COOH CdSe/ZnS 525, COOH CdSe/ZnS 625, NH_2 CdSe/ZnS 525, and NH_2 CdSe/ZnS 625 by *P. chrysosporium* incubated with different concentrations for 24 h. (a) CdSe/ZnS QDs, calculated from Cd; (b) CdSe/ZnS QDs, calculated from Se. Correlation between QD uptake and incubation concentration in the medium. (c) CdSe/ZnS QDs, calculated from Cd; (d) CdSe/ZnS QDs, calculated from Se. Error bars represent one standard deviation of the arithmetic mean.

625 during the 24 h period is depicted in Fig. 3. As shown in Fig. 3a, the uptake by *P. chrysosporium* increased with incubation time for all four types of CdSe/ZnS QDs since the accumulation of CdSe/ZnS QDs in *P. chrysosporium* presented a time-dependent process. However, the cellular uptake of different CdSe/ZnS QDs was obviously different under identical conditions. For example, the cellular uptake of NH_2 CdSe/ZnS 525 reached 299.7 pmol g^{-1} biomass at 24 h when the incubation concentration was 80 nM, which was greater than those of NH_2 CdSe/ZnS 625 (171.2 pmol g^{-1} biomass), COOH CdSe/ZnS 525 (105.6 pmol g^{-1} biomass), and COOH CdSe/ZnS 625 (72.3 pmol g^{-1} biomass), and the increase rate of NH_2 CdSe/ZnS 525 was the largest. The cellular uptake of CdSe/ZnS QDs presented a time-dependent saturation, that is to say that the uptake amount of CdSe/ZnS QDs finally achieved a plateau. This is because the cellular uptake process of CdSe/ZnS QDs included the binding of CdSe/ZnS QDs to receptors on the plasma membrane surface and the generation of coated pits to deliver them to the intracellular area.[45] The amount of receptors on the plasma membrane surface would determine the uptake of CdSe/ZnS QDs, and the membrane receptors were gradually consumed as time lapsed.[45] Therefore, the internalization rate of CdSe/ZnS QDs would decline and eventually reach equilibrium. In addition, the smaller size and less negative charges make it easier and faster for NH_2 CdSe/ZnS 525 to be internalized by *P. chrysosporium*.[44] As shown in Fig. 3b, the same results were also observed by determining the Se concentration.

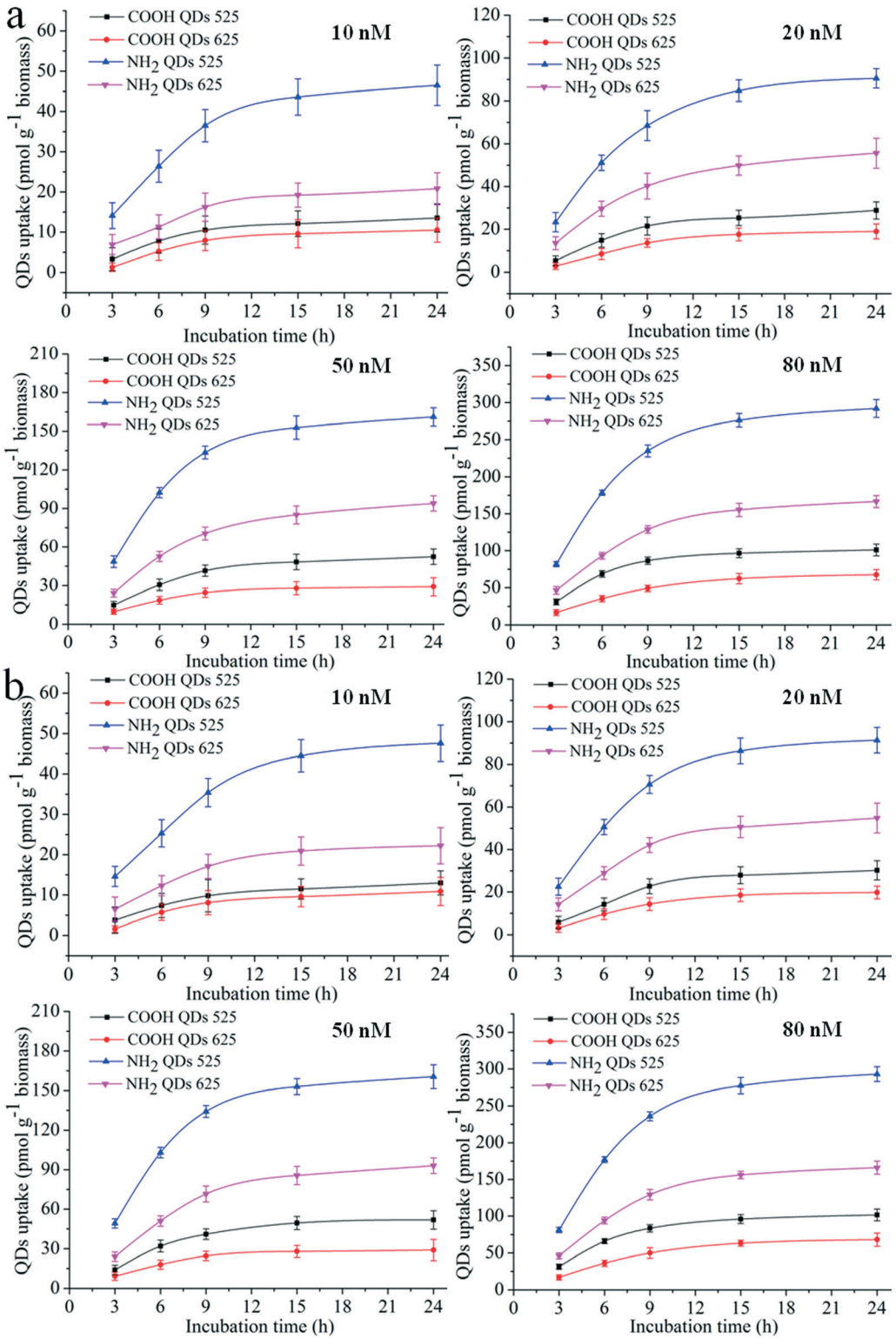

Fig. 3 Cellular uptake of COOH CdSe/ZnS 525, COOH CdSe/ZnS 625, NH_2 CdSe/ZnS 525, and NH_2 CdSe/ZnS 625 by *P. chrysosporium* incubated for different times. Initial CdSe/ZnS QD concentrations are 10, 20, 50, and 80 nM, respectively. (a) CdSe/ZnS QDs, calculated from Cd; (b) CdSe/ZnS QDs, calculated from Se. Error bars represent one standard deviation of the arithmetic mean.

3.3. Confocal laser scanning microscopy analysis

To investigate the intracellular distribution of CdSe/ZnS QDs, the localization of CdSe/ZnS QDs in the hyphae of *P. chrysosporium* was analyzed by confocal laser scanning microscopy. As shown in Fig. 4, the green fluorescence channels represent the hyphae of *P. chrysosporium*, in which all

the four types of CdSe/ZnS QDs largely accumulated. When CdSe/ZnS QDs entered into the hyphae and accumulated largely in the hyphae of *P. chrysosporium*, ROS were subsequently generated *in vivo*. Therefore, the generation of intracellular ROS was qualitatively analyzed by confocal laser scanning microscopy coupled with H_2DCF-DA assay to explore the potential roles of CdSe/ZnS QDs in inducing intracellular oxidative stress. It can be seen from Fig. 4 that the existence of fluorescence indicated the generation of ROS in the hyphae of *P. chrysosporium*, and all the samples presented significant differences as compared to the control. These phenomena suggest that CdSe/ZnS QDs accumulated largely in the hyphae of *P. chrysosporium*, and the accumulated CdSe/ZnS QDs had induced the generation of ROS and caused oxidative stress in *P. chrysosporium*. Oxidative stress is one of the significant mechanisms of QD cytotoxicity.[46,47] The intracellular ROS would disturb the redox potential equilibrium, leading to an intracellular pro-oxidant environment, and ultimately cause the disruption of cell function.[46,48]

3.4. CdSe/ZnS QD-induced oxidative stress in *P. chrysosporium*

3.4.1. Lipid peroxidation and superoxide (O_2^-) production. MDA is generally used as an indicator of free radical production and a cytotoxic product of lipid peroxidation.[35,49] In order to evaluate the CdSe/ZnS QD-induced oxidative stress in *P. chrysosporium*, the MDA content and O_2^- level in *P. chrysosporium* exposed to four types of CdSe/ZnS QDs were measured under different incubation concentrations. As

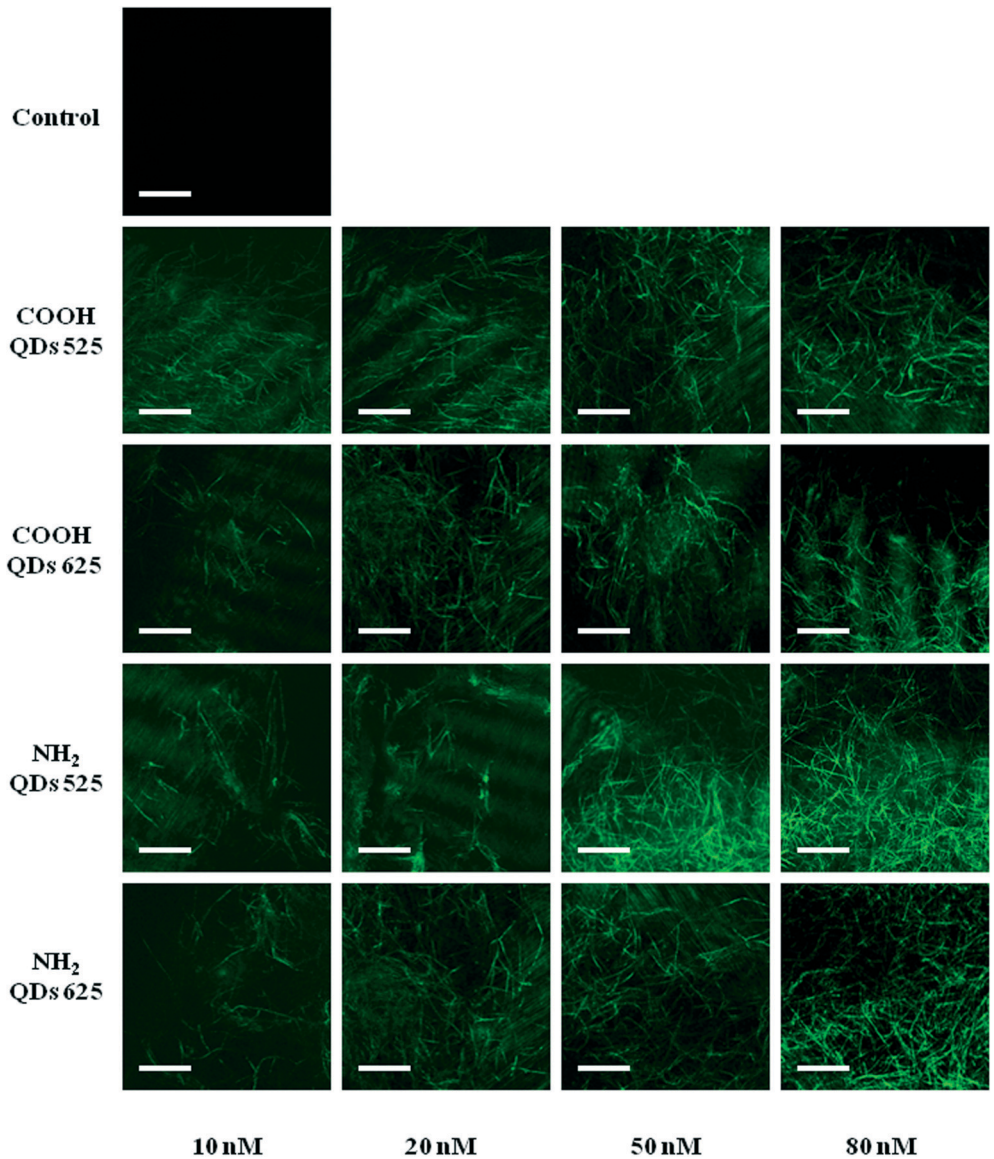

Fig. 4 Confocal laser scanning microscopy images of the hyphal localization (green fluorescence channel) of COOH CdSe/ZnS 525, COOH CdSe/ZnS 625, NH_2 CdSe/ZnS 525, and NH_2 CdSe/ZnS 625. Their initial concentrations are 10, 20, 50, and 80 nM, respectively. The control group was the *P. chrysosporium* pellets without CdSe/ZnS QD exposure. Scale bars are 10 μm.

shown in Fig. 5a, the MDA content in *P. chrysosporium* increased obviously with incubation concentrations for all four types of CdSe/ZnS QDs. And the MDA content presented a significant increase as compared to the control under various concentrations. However, the MDA contents for different CdSe/ZnS QDs exposures were distinctly different under identical concentrations. For example, the MDA content for NH_2 CdSe/ZnS 525 exposure reached 8.521×10^{-6} mol g^{-1} when the incubation concentration was 80 nM, which was greater than those of NH_2 CdSe/ZnS 625 (6.952×10^{-6} mol g^{-1}), COOH CdSe/ZnS 525 (5.723×10^{-6} mol g^{-1}), COOH CdSe/ZnS 625 (4.472×10^{-6} mol g^{-1}), and the control (0.856×10^{-6} mol g^{-1}). This result may be related to the cellular uptake of NH_2 CdSe/ZnS 525 being the greatest. The increased MDA content showed that CdSe/ZnS QDs have stimulated the generation of free radicals in *P. chrysosporium*. When CdSe/ZnS QDs entered into *P. chrysosporium*, they could inhibit the mitochondrial electron-transfer chain, resulting in the accumulation of semi-ubiquinone, which enabled the transfer of one electron to molecular oxygen (O_2) to form a superoxide radical (O_2^-).[50] The generation of free radicals, in turn, led to lipid peroxidation.[51] Thus, the MDA content is associated with the production of O_2^-. As shown in Fig. 5b, the O_2^- level in *P. chrysosporium* exposed to four types of CdSe/ZnS QDs was similar to that of MDA, as described above. When *P. chrysosporium* was incubated with 80 nM CdSe/ZnS QDs for 24 h, the O_2^- level for NH_2 CdSe/ZnS 525 exposure reached 13.635×10^{-6} mol g^{-1}, which was greater than those of NH_2 CdSe/ZnS 625 (10.152×10^{-6} mol g^{-1}), COOH CdSe/ZnS 525 (8.823×10^{-6} mol g^{-1}), COOH CdSe/ZnS 625 (7.042×10^{-6} mol g^{-1}), and the control (3.213×10^{-6} mol g^{-1}). The increased O_2^- level is known to be a significant factor causing the cytotoxicity of CdSe/ZnS QDs since O_2^- has been proved to cause metabolic functions loss, DNA nicking and breakage, and apoptosis.[15] Therefore, the above results indicated that all four types of CdSe/ZnS QDs showed cytotoxicity to *P. chrysosporium* in the tested concentration range (10–80 nM).

3.4.2. Antioxidant enzymes analysis. Antioxidant enzymes have been considered as the defenders in response to oxidative stress.[52–54] In this study, two antioxidant enzymes, namely, SOD and CAT, have been monitored under different CdSe/ZnS QD concentrations. As shown in Fig. 5c, the activity of SOD in *P. chrysosporium* increased gradually with incubation concentration for all four types of CdSe/ZnS QDs. And the SOD activity presented a significant increase as compared to the control under various concentrations. However, the SOD activities for different CdSe/ZnS QD exposures were distinctly different under identical concentrations. For example, the SOD activity for NH_2 CdSe/ZnS 525 exposure reached 9.235 U g^{-1} when the incubation concentration was 80 nM, which was greater than those of NH_2 CdSe/ZnS 625 (7.652 U g^{-1}), COOH CdSe/ZnS 525 (6.323 U g^{-1}), COOH CdSe/ZnS 625 (5.862 U g^{-1}), and the control (2.304 U g^{-1}). The SOD activity decreased as follows: NH_2 CdSe/ZnS 525 > NH_2 CdSe/ZnS

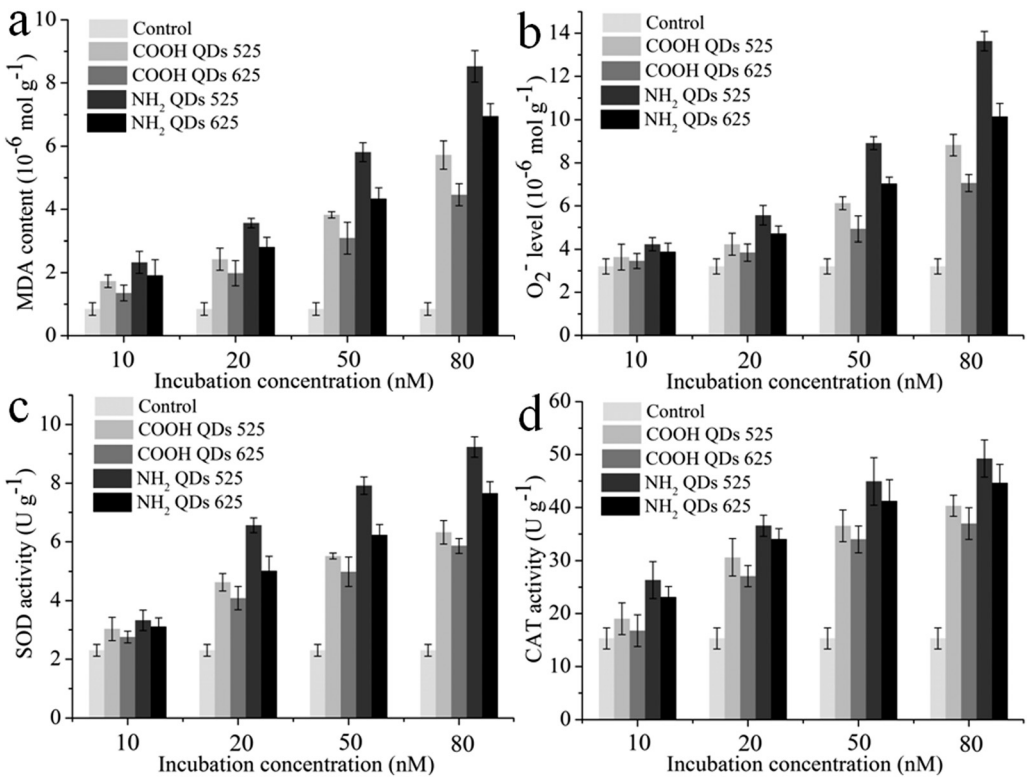

Fig. 5 Oxidative stress in *P. chrysosporium* after exposure to COOH CdSe/ZnS 525, COOH CdSe/ZnS 625, NH_2 CdSe/ZnS 525, and NH_2 CdSe/ZnS 625 with different concentrations for 24 h. The control group was the *P. chrysosporium* pellets without CdSe/ZnS QD exposure. (a) MDA content, (b) O_2^- level, (c) SOD activity, and (d) CAT activity. Error bars represent one standard deviation of the arithmetic mean.

625 > COOH CdSe/ZnS 525 > COOH CdSe/ZnS 625 > control, which suggested that NH_2 CdSe/ZnS 525 could induce greater oxidative stress in *P. chrysosporium* than the other three types of CdSe/ZnS QDs. Similarly, this result may be ascribed to the greater cellular uptake of NH_2 CdSe/ZnS 525 since a large amount of NH_2 CdSe/ZnS 525 in *P. chrysosporium* would lead to the accumulation of ROS.[30] The increased SOD activity was the physiological response of *P. chrysosporium* to eliminate ROS and relieve oxidative stress. As shown in Fig. 5d, the activity of CAT in *P. chrysosporium* exposed to four types of CdSe/ZnS QDs was similar to that of SOD, as described above. When *P. chrysosporium* was incubated with 80 nM CdSe/ZnS QDs for 24 h, the CAT activity for NH_2 CdSe/ZnS 525 exposure reached 49.250 U g^{-1}, which was greater than those of NH_2 CdSe/ZnS 625 (44.682 U g^{-1}), COOH CdSe/ZnS 525 (40.363 U g^{-1}), COOH CdSe/ZnS 625 (36.964 U g^{-1}), and the control (15.324 U g^{-1}). Therefore, the induction of antioxidant enzyme (SOD and CAT) activity is essential for *P. chrysosporium* to obtain the ability to relieve oxidative stress to some extent. Peng *et al.*[47] have reported that antioxidant enzyme production might be a defense mechanism, since it provided a powerful defense against CdSe/ZnS QD cytotoxicity before the induction of metallothionein synthesis.

3.4.3. Linear analysis of cytotoxicity response and CdSe/ZnS QD concentrations. To explore the effect of CdSe/ZnS QD exposure on *P. chrysosporium*, a linear analysis was used to reveal the relationship between the cytotoxicity response of *P. chrysosporium* and CdSe/ZnS QD concentrations. As depicted in Fig. 6a, the MDA content, O_2^- level, SOD activity and CAT activity increased gradually with an increase of COOH CdSe/ZnS 525 concentration, indicating that the MDA content, O_2^-

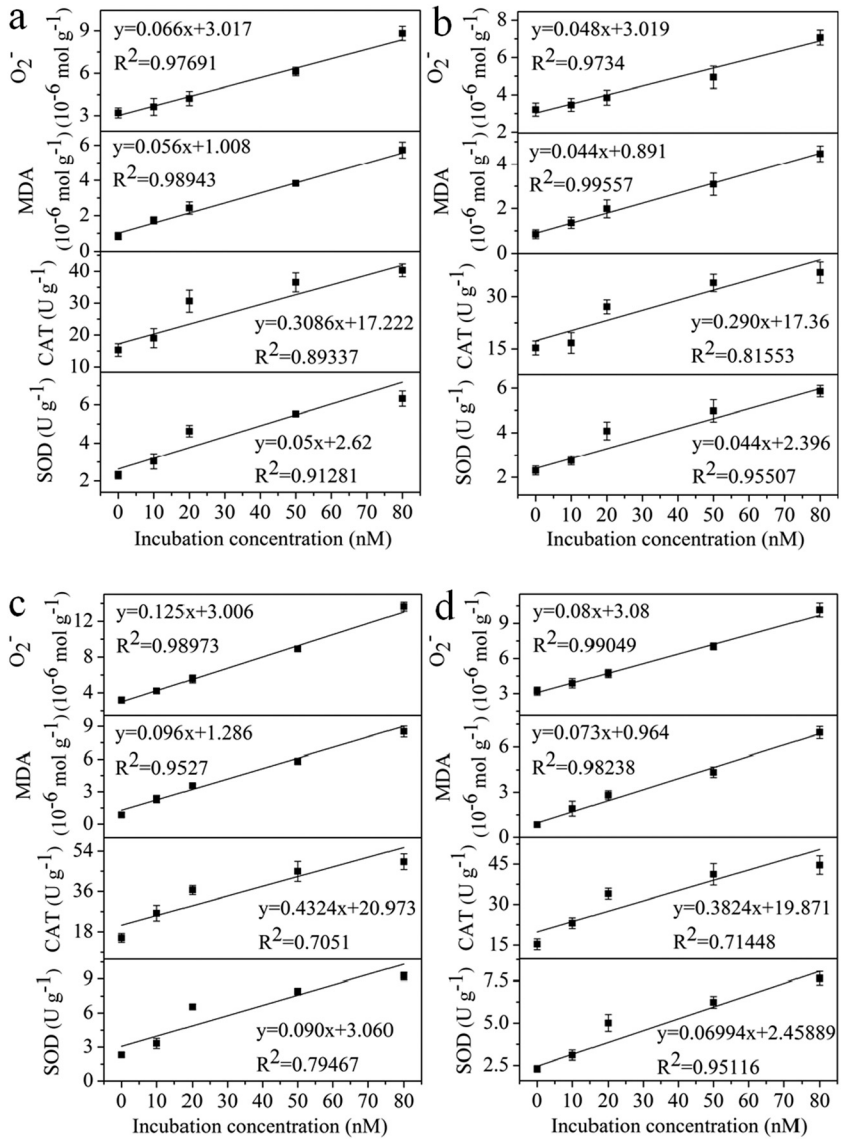

Fig. 6 Correlation between cytotoxicity response (MDA content, O_2^- level, SOD activity, and CAT activity) and CdSe/ZnS QD concentration in the medium. (a) COOH CdSe/ZnS 525, (b) COOH CdSe/ZnS 625, (c) NH_2 CdSe/ZnS 525, and (d) NH_2 CdSe/ZnS 625. R^2 represents the linearly dependent coefficient. Error bars represent one standard deviation of the arithmetic mean.

level, SOD activity and CAT activity were dose-dependent and the cellular uptake of COOH CdSe/ZnS 525 increased with incubation concentration. Similar results can be observed in Fig. 6b–d. However, there are also some differences among the four types of CdSe/ZnS QDs. For example, the MDA content and O_2^- level correlated well (R^2 = 0.98943 and R^2 = 0.97691, respectively) with the concentration of COOH CdSe/ZnS 525 but not the SOD activity and CAT activity (R^2 = 0.91281 and R^2 = 0.89337, respectively). The MDA content, O_2^- level and SOD activity correlated well (R^2 = 0.99557, R^2 = 0.97340 and R^2 = 0.95507, respectively) with the concentration of COOH CdSe/ZnS 625 but not the CAT activity (R^2 = 0.81553). The MDA content and O_2^- level correlated well (R^2 = 0.95270 and R^2 = 0.98973, respectively) with the concentration of NH_2 CdSe/ZnS 525 but not the SOD activity and CAT activity (R^2 = 0.79467 and R^2 = 0.70510, respectively). The MDA content, O_2^- level and SOD activity correlated well (R^2 = 0.98238, R^2 = 0.99049 and R^2 = 0.95116, respectively) with the concentration of NH_2 CdSe/ZnS 625 but not the CAT activity (R^2 = 0.71448). The antioxidant enzymes (SOD and CAT) are produced to protect the cellular components from damage under CdSe/ZnS QD-induced oxidative stress. However, when the induced oxidative stress exceeds the scavenging ability of the antioxidant enzymes, cellular damage would occur, as confirmed by the decreased correlation between SOD and CAT activity and CdSe/ZnS QD concentrations. These phenomena are in accordance with the findings reported by Chen *et al.*[30] who described the stress responses of *P. chrysosporium* under cadmium exposure and considered the slowly increased part as an exhaustion stage in which the defense systems were overloaded, resulting in chronic damage and cell death.

3.4.4. Glutathione levels. GSH is a significant antioxidant and can scavenge oxygen free radicals, and it plays an important role in the detoxification of exogenous chemicals.[22] In order to investigate the CdSe/ZnS QD-induced oxidative stress in *P. chrysosporium*, the GSH content in *P. chrysosporium* exposed to four types of CdSe/ZnS QDs was measured under different incubation concentrations. As shown in Fig. 7, within the concentration range of 10–80 nM, there was an obvious reduction of GSH content in *P. chrysosporium* after incubation with all four types of CdSe/ZnS QDs. And the GSH content decreased significantly as compared to the control under various concentrations. However, when *P. chrysosporium* was incubated with 80 nM CdSe/ZnS QDs for 24 h, the GSH content for NH_2 CdSe/ZnS 525 exposure was 41.5% that of the control, which was lower than those of NH_2 CdSe/ZnS 625 (56.2% that of the control), COOH CdSe/ZnS 525 (63.3% that of the control), and COOH CdSe/ZnS 625 (75.6% that of the control). The results showed that NH_2 CdSe/ZnS 525 has induced greater oxidative stress in *P. chrysosporium* than the other three types of CdSe/ZnS QDs. The decreased GSH content is most probably attributed to the depletion of GSH in the scavenging of ROS,[55] which indicated the importance of GSH in detoxification and the ability of *P. chrysosporium* to tolerate CdSe/ZnS QD exposure. The results are consistent with the report of Peng *et al.*[22] who demonstrated direct evidence for the involvement of GSH in CdSe/ZnS QD detoxification in HepG2 cells.

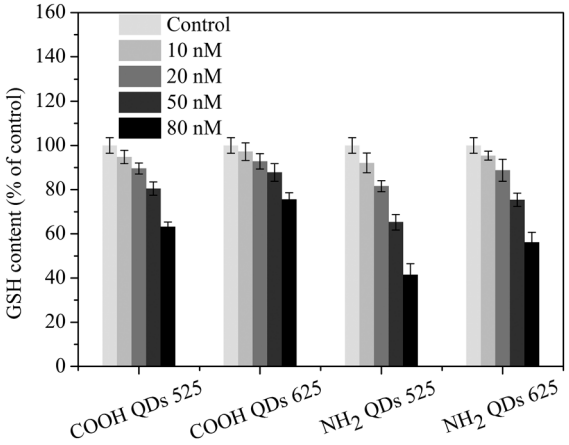

Fig. 7 The variation of GSH content in *P. chrysosporium* after exposure to COOH CdSe/ZnS 525, COOH CdSe/ZnS 625, NH_2 CdSe/ZnS 525, and NH_2 CdSe/ZnS 625 with different concentrations for 24 h. The control group was the *P. chrysosporium* pellets without CdSe/ZnS QD exposure. Error bars represent one standard deviation of the arithmetic mean.

4. Conclusions

This work comprehensively investigated the cellular uptake of four CdSe/ZnS QDs and induced physiological responses in *P. chrysosporium via* ICP-OES, confocal laser scanning microscopy, and the analyses of MDA content, O_2^- level, SOD activity, CAT activity and GSH level. According to the results of ICP-OES, we found that negatively charged CdSe/ZnS QDs with small size were more easily taken in by *P. chrysosporium* than large ones. Meanwhile, four CdSe/ZnS QDs accumulated largely in the hyphae and caused oxidative stress to *P. chrysosporium* in the tested concentration range. The MDA content, O_2^- level, SOD activity, CAT activity and GSH level analysis results showed that CdSe/ZnS QDs with small size were more cytotoxic than CdSe/ZnS QDs with large size, and small negatively charged CdSe/ZnS QDs resulted in greater cytotoxicity than large negatively charged CdSe/ZnS QDs. Further studies are urgently necessary to elucidate the underlying toxicity mechanism, which will eventually be used to prevent the adverse impacts of QDs in clinical application.

Conflicts of interest

There are no conflicts of interest to declare.

Acknowledgements

This work was financially supported by the National Natural Science Foundation of China (51521006, 51579099, 51508186, and 51378190), the Program for Changjiang Scholars and Innovative Research Team in University (IRT-13R17) and the

Hunan Provincial Natural Science Foundation of China (2015JJ2031 and 2016JJ3076).

References

1 W. C. Chan, D. J. Maxwell, X. Gao, R. E. Bailey, M. Han and S. Nie, *Curr. Opin. Biotechnol.*, 2002, **13**, 40–46.
2 M. Chu, X. Pan, D. Zhang, Q. Wu, J. Peng and W. Hai, *Biomaterials*, 2012, **33**, 7071–7083.
3 Y. Zhang, G. M. Zeng, L. Tang, D. L. Huang, X. Y. Jiang and Y. N. Chen, *Biosens. Bioelectron.*, 2007, **22**, 2121–2126.
4 X. Michalet, F. Pinaud, L. Bentolila, J. Tsay, S. Doose, J. Li, G. Sundaresan, A. Wu, S. Gambhir and S. Weiss, *Science*, 2005, **307**, 538–544.
5 I. L. Medintz, H. T. Uyeda, E. R. Goldman and H. Mattoussi, *Nat. Mater.*, 2005, **4**, 435–446.
6 H. Wang, X. Z. Yuan, Y. Wu, X. H. Chen, L. J. Leng and G. M. Zeng, *RSC Adv.*, 2015, **5**, 32531–32535.
7 H. Wang, X. Z. Yuan, H. Wang, X. H. Chen, Z. B. Wu, L. B. Jiang, W. P. Xiong and G. M. Zeng, *Appl. Catal., B*, 2016, **193**, 36–46.
8 Z. Z. Wu, X. Z. Yuan, H. Wang, Z. B. Wu, L. B. Jiang, H. Wang, L. Zhang, Z. H. Xiao, X. H. Chen and G. M. Zeng, *Appl. Catal., B*, 2017, **202**, 104–111.
9 L. Hu, C. Zhang, G. Zeng, G. Chen, J. Wan, Z. Guo, H. Wu, Z. Yu, Y. Zhou and J. Liu, *RSC Adv.*, 2016, **6**, 78595–78610.
10 D. Mo, L. Hu, G. Zeng, G. Chen, J. Wan, Z. Yu, Z. Huang, K. He, C. Zhang and M. Cheng, *Appl. Microbiol. Biotechnol.*, 2017, **101**, 2713–2733.
11 L. Tang, G. M. Zeng, G. L. Shen, Y. P. Li, Y. Zhang and D. L. Huang, *Environ. Sci. Technol.*, 2008, **42**, 1207–1212.
12 M. D. Peterson, S. C. Jensen, D. J. Weinberg and E. A. Weiss, *ACS Nano*, 2014, **8**, 2826–2837.
13 N. A. Al-Hajaj, A. Moquin, K. D. Neibert, G. M. Soliman, F. O. M. Winnik and D. Maysinger, *ACS Nano*, 2011, **5**, 4909–4918.
14 Y. H. Luo, S. B. Wu, Y. H. Wei, Y. C. Chen, M. H. Tsai, C. C. Ho, S. Y. Lin, C. S. Yang and P. Lin, *Chem. Res. Toxicol.*, 2013, **26**, 662–673.
15 A. Nagy, A. Steinbrück, J. Gao, N. Doggett, J. A. Hollingsworth and R. Iyer, *ACS Nano*, 2012, **6**, 4748–4762.
16 G. Zeng, M. Chen and Z. Zeng, *Nature*, 2013, **499**, 154.
17 P. Rivera-Gil, D. Jimenez De Aberasturi, V. Wulf, B. Pelaz, P. Del Pino, Y. Zhao, J. M. De La Fuente, I. Ruiz De Larramendi, T. Rojo and X. J. Liang, *Acc. Chem. Res.*, 2012, **46**, 743–749.
18 H. Li, M. Li, W. Y. Shih, P. I. Lelkes and W. H. Shih, *J. Nanosci. Nanotechnol.*, 2011, **11**, 3543–3551.
19 Y. Su, Y. He, H. Lu, L. Sai, Q. Li, W. Li, L. Wang, P. Shen, Q. Huang and C. Fan, *Biomaterials*, 2009, **30**, 19–25.
20 R. F. Domingos, D. F. Simon, C. Hauser and K. J. Wilkinson, *Environ. Sci. Technol.*, 2011, **45**, 7664–7669.
21 S. J. Soenen, J. Demeester, S. C. De Smedt and K. Braeckmans, *Biomaterials*, 2012, **33**, 4882–4888.
22 L. Peng, M. He, B. Chen, Q. Wu, Z. Zhang, D. Pang, Y. Zhu and B. Hu, *Biomaterials*, 2013, **34**, 9545–9558.
23 A. Hoshino, S. Hanada and K. Yamamoto, *Arch. Toxicol.*, 2011, **85**, 707.
24 P. Xu, G. M. Zeng, D. L. Huang, C. L. Feng, S. Hu, M. H. Zhao, C. Lai, Z. Wei, C. Huang and G. X. Xie, *Sci. Total Environ.*, 2012, **424**, 1–10.
25 C. Yang, H. Chen, G. Zeng, G. Yu and S. Luo, *Biotechnol. Adv.*, 2010, **28**, 531–540.
26 T. Fan, Y. Liu, B. Feng, G. Zeng, C. Yang, M. Zhou, H. Zhou, Z. Tan and X. Wang, *J. Hazard. Mater.*, 2008, **160**, 655–661.
27 D. L. Huang, G. M. Zeng, C. L. Feng, S. Hu, X. Y. Jiang, L. Tang, F. F. Su, Y. Zhang, W. Zeng and H. L. Liu, *Environ. Sci. Technol.*, 2008, **42**, 4946–4951.
28 Y. Feng, J. L. Gong, G. M. Zeng, Q. Y. Niu, H. Y. Zhang, C. G. Niu, J. H. Deng and M. Yan, *Chem. Eng. J.*, 2010, **162**, 487–494.
29 G. Zeng, M. Chen and Z. Zeng, *Science*, 2013, **340**, 1403.
30 A. Chen, G. Zeng, G. Chen, L. Liu, C. Shang, X. Hu, L. Lu, M. Chen, Y. Zhou and Q. Zhang, *Process Biochem.*, 2014, **49**, 589–598.
31 L. Hu, G. Zeng, G. Chen, H. Dong, Y. Liu, J. Wan, A. Chen, Z. Guo, M. Yan and H. Wu, *J. Hazard. Mater.*, 2016, **301**, 106–118.
32 J. L. Gong, B. Wang, G. M. Zeng, C. P. Yang, C. G. Niu, Q. Y. Niu, W. J. Zhou and Y. Liang, *J. Hazard. Mater.*, 2009, **164**, 1517–1522.
33 Y. He, H. T. Lu, L. M. Sai, Y. Y. Su, M. Hu, C. H. Fan, W. Huang and L. H. Wang, *Adv. Mater.*, 2008, **20**, 3416–3421.
34 T. K. Kirk, E. Schultz, W. Connors, L. Lorenz and J. Zeikus, *Arch. Microbiol.*, 1978, **117**, 277–285.
35 G. M. Zeng, A. W. Chen, G. Q. Chen, X. J. Hu, S. Guan, C. Shang, L. H. Lu and Z. J. Zou, *Environ. Sci. Technol.*, 2012, **46**, 7818–7825.
36 P. Aravind and M. N. V. Prasad, *Plant Physiol. Biochem.*, 2003, **41**, 391–397.
37 Y. Lei, C. Yin and C. Li, *Physiol. Plant.*, 2006, **127**, 182–191.
38 F. R. Cavalcanti, J. T. A. Oliveira, A. S. Martins-Miranda, R. A. Viégas and J. A. G. Silveira, *New Phytol.*, 2004, **163**, 563–571.
39 A. Rehman and M. S. Anjum, *Environ. Monit. Assess.*, 2011, **174**, 585–595.
40 Y. Su, F. Peng, Z. Jiang, Y. Zhong, Y. Lu, X. Jiang, Q. Huang, C. Fan, S. T. Lee and Y. He, *Biomaterials*, 2011, **32**, 5855–5862.
41 X. J. Hu, J. S. Wang, Y. G. Liu, X. Li, G. M. Zeng, Z. L. Bao, X. X. Zeng, A. W. Chen and F. Long, *J. Hazard. Mater.*, 2011, **185**, 306–314.
42 Z. Huang, G. Chen, G. Zeng, Z. Guo, K. He, L. Hu, J. Wu, L. Zhang, Y. Zhu and Z. Song, *J. Hazard. Mater.*, 2017, **321**, 37–46.
43 S. Zhang, Y. Jiang, C. S. Chen, J. Spurgin, K. A. Schwehr, A. Quigg, W. C. Chin and P. H. Santschi, *Environ. Sci. Technol.*, 2012, **46**, 8764–8772.
44 X. Jiang, C. Röcker, M. Hafner, S. Brandholt, R. M. Dörlich and G. U. Nienhaus, *ACS Nano*, 2010, **4**, 6787–6797.
45 S. Ohta, S. Inasawa and Y. Yamaguchi, *Biomaterials*, 2012, **33**, 4639–4645.

46 E. Q. Contreras, M. Cho, H. Zhu, H. L. Puppala, G. Escalera, W. Zhong and V. L. Colvin, *Environ. Sci. Technol.*, 2013, **47**, 1148.
47 L. Peng, M. He, B. Chen, Y. Qiao and B. Hu, *ACS Nano*, 2015, **9**, 10324–10334.
48 J. Wan, G. Zeng, D. Huang, C. Huang, C. Lai, N. Li, Z. Wei, P. Xu, X. He and M. Lai, *Appl. Biochem. Biotechnol.*, 2015, **175**, 1981–1991.
49 J. Wan, C. Zhang, G. Zeng, D. Huang, L. Hu, C. Huang, H. Wu and L. Wang, *J. Hazard. Mater.*, 2016, **320**, 278–288.
50 S. Garg, H. Rong, C. J. Miller and T. D. Waite, *Environ. Sci. Technol.*, 2016, **50**, 3890–3896.
51 Y. Lu, S. Xu, H. Chen, M. He, Y. Deng, Z. Cao, H. Pi, C. Chen, M. Li and Q. Ma, *Biomaterials*, 2016, **90**, 27–39.
52 R. Liu, H. H. Liu, Z. Ji, C. H. Chang, T. Xia, A. E. Nel and Y. Cohen, *ACS Nano*, 2015, **9**, 9303–9313.
53 Y. Cheng, H. He, C. Yang, G. Zeng, X. Li, H. Chen and G. Yu, *Biotechnol. Adv.*, 2016, **34**, 1091–1102.
54 G. M. Zeng, J. Wan, D. L. Huang, L. Hu, C. Huang, M. Cheng, W. J. Xue, X. M. Gong, R. Z. Wang and D. N. Jiang, *J. Hazard. Mater.*, 2017, **339**, 354–367.
55 Y. Matsufuji, K. Yamamoto, K. Yamauchi, T. Mitsunaga, T. Hayakawa and T. Nakagawa, *Appl. Microbiol. Biotechnol.*, 2013, **97**, 297–303.